

CENOMANIAN RAMP (GALALA FORMATION), NORTH EASTERN DESERT, EGYPT: FACIES ARCHITECTURE AND DEPOSITIONAL HISTORY

M. A. Khalifa*, Mohamed S. Abu El Ghar**, Sobhi A. Helal** & Ahmed W. Hussein**

*Faculty of Science, Menoufia University, Shibeen El-Kom, Egypt

**Faculty of Science Fayoum University, Fayoum, Egypt

msa02@fayoum.edu.eg

ABSTRACT

The Cenomanian Galala Formation is composed of a thick mixed siliciclastic-carbonate facies outcropping in the north Eastern Desert, Egypt. It was deposited on a passive continental margin of southern Tethys. It displays a lateral facies changes in the form of a homoclinal ramp that is divided into two environmental settings; proximal and middle ramp. The proximal ramp is characterized by the siliciclastic-dominated coastal marine shoreface to peritidal facies and the mixed siliciclastic-carbonate intertidal-supratidal facies. The middle ramp includes three facies types; the peritidal, shallow subtidal and deep subtidal facies. The facies distribution on the middle ramp points out to that the ramp was drowned under the effect of local tectonic subsidence due to the east-west Tethyan tectonic movements during the Jurassic rifting forming an intra-ramp basin at the Southern Galala. The dominance of the carbonate facies in the northern part of the study area reflects that it was subjected to structural uplifting under the effect of the Syrian Arc System to form a carbonate buildup at Gebel Ataqa.

INTRODUCTION

Ahr (1973) defined the ramp as a carbonate platform that is characterized by having no pronounced break in slope from the coastline to the deep water. Markello and Read (1981) subdivided the ramp system in southeast Virginia Appalachian into three zones; the peritidal carbonate platform (shallow subtidal to supratidal), shallow ramp (ooid sand shoal, above the fair weather wave base) and deep ramp (ribbon limestone lithotope, below the fair weather wave base). Read (1985) gave two types of ramps; the homoclinal and the distally steepened ramp. He (op.cit) stated that the lack of the reefs is a characteristic feature of ramps. Wright (1986) classified the carboniferous ramp of South Wales into three zones; the inner ramp zone dominated by oolitic grainstones and peritidal facies, the mid ramp zone of bioclastic limestones below the fair weather wave base and the outer ramp zone that consists mainly of muddy bioclastic limestones developed below the storm wave base. Burchette and Wright (1992) subdivided the carbonate homoclinal ramp environments into three settings; the inner ramp (shoreface, sand shoals or organic barriers and peritidal facies deposited above the fair-weather wave base), the mid-ramp (between the fair weather wave base and the storm wave base) and the outer ramp (below the storm wave base). Tucker et al. (1993) categorized the carbonate ramps into three regions; the back ramp, shallow ramp and the deep ramp. Keller (1997) documented that the homoclinal ramp facies are dominated by tidal flat deposits with oolitic shoals and bioclastic limestones.

The Galala Formation (Cenomanian) represents a ramp model that displays a change in facies from south to north. It occurs in dissected localities, in the north Eastern Desert, separated by east-west faults as found in Gebel El-Zeit, Southern and Northern Galalas, Gebel Ataqa and Gebel Shabraweet. In spite of the Galala Formation was studied in detail by numerous geologists concerning the sedimentological and paleontological (e.g. El-Akkad and Abdallah 1971; Al-Ahwani 1982; Metwally et al. 1995; Abdel Shafy et al. 2002; Khalifa and Kandil 2004, Abdel Gawad et al. 2007, Khalifa and El-Ayyat 2007 and El-Ayyat and Khalifa 2010), the regional vertical and lateral facies changes associated with tectonic movements still need more investigation.

The main aims of this study are: 1). to determine the lithofacies distribution of the Cenomanian Galala Formation from south to north to predict the changes in depositional environments. 2). to suggest the depositional evolution of the ramp facies of the Galala Formation; 3). to reconstruct the paleo-tectonic configuration, dominated meanwhile the sedimentation period during the Cenomanian time. 4). to propose the depositional history of the Galala Formation.

Geological Setting

The north Eastern Desert of Egypt is situated at the northern edge of the African-Arabian Craton and was subjected to tectonic movements during the Late Cretaceous-Early Tertiary by east-northeast-oriented dextral wrench faulting (Kuss et al. 2000). Alpine Orogeny was a consequence of the collision between the African and European plates. It was resulted in the closure of the Tethys and development of an overall pulsed compressional regime across North Africa from mid Cretaceous to recent time (Bosworth et al. 1999). The Syrian Arc system may be considered as a phase of the Alpine Orogeny that affected the Upper Cretaceous sediments in the Eastern Desert. The Upper Cretaceous sedimentary rocks in the northeastern Desert of Egypt were affected by the Syrian Arc System that dominated from Late Cretaceous up to the Early Tertiary times (Guiraud and Bosworth 1997 and Bosworth et al. 1999). The anticlinal folding structures that characterize the Syrian Arc fold belt were formed during the closure of the Neo-Tethys as a result of the convergence of the African and Eurasian plates. It was affected by the reactivated deep-seated faults that dominated during Late Triassic-Early Jurassic, accompanied with the opening of the Neo-Tethys (Kuss 1992 and El-Hawat 1997).

In general, it is accepted that the major tectonic movements were started in the Late Cretaceous, but the timing of first compressional pulses is a subject of many debates among geologists, that may range from Cenomanian to Campanian. Differential subsidence along reactivated deep seated faults during the Late Cenomanian in the north Eastern Desert may correspond with similar structural features in other adjacent localities in Sinai (Bauer et al. 2003) and in northern Africa (Camion 1991).

The Cenomanian facies in Egypt were deposited under two realms on the continental passive margin; the southern realm (or southern facies belt) and the northern realm (or northern facies belt). The southern realm is represented by the deposits on the southern part of the passive margin; this may equivalent to the stable shelf of Said (1962) that includes the siliciclastic facies of the Maghrabi Formation (Barthel and Hermann-Degen 1981) in the in south Western Desert (Dakhla and Kharga Oases), the Bahariya Formation (Said 1962) in the north Western Desert and the Raha Formation in southern Sinai (Ghorab 1961). The northern realm is manifested by the mixed clastic-carbonate facies that deposited on the northern part of the passive margin; this may equivalent to the unstable shelf of Said (1962). This realm includes Abu Roash Formation (Norton 1967) in the north Western Desert and the Halal Formation in north Sinai (Said 1971)

The Cenomanian Galala Formation covers part of the southern facies belt at Gebel El-Zeit and Southern and Northern Galalas, where it consists mainly of siliciclastic-dominated facies. Gebel Ataqa and Gebel Shabraweet lie within the northern facies belt, where the carbonate facies dominated over the siliciclastics with a marked increased thickness (Fig.1).

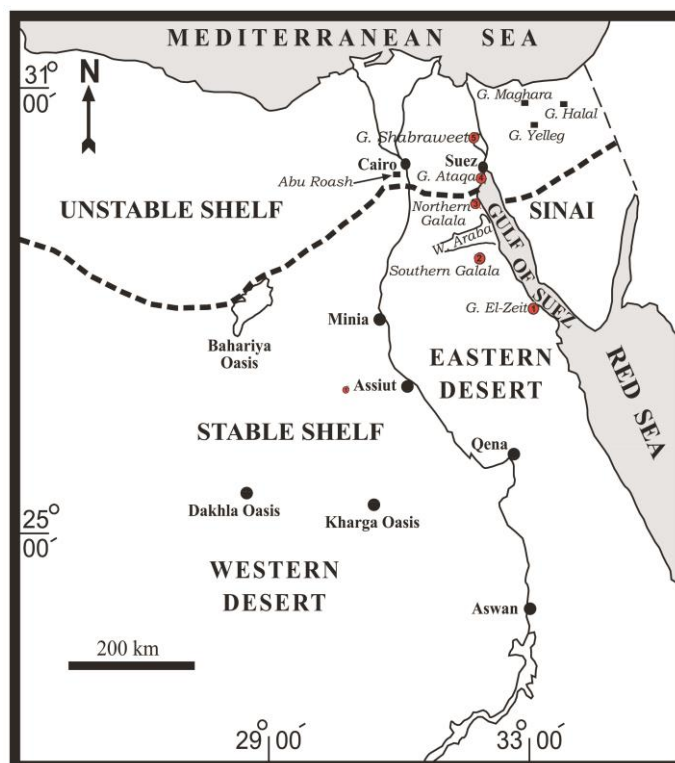


Fig.1: A simplified and location map of Egypt shows the distribution of the stable and unstable shelves and the position of the studied sections within them. Notice: the heavy dashed line marks the separation between the stable and unstable shelves.

Methods of Study

To accomplish the target of this study, the following steps were executed: 1). a detailed field work was carried out, including measuring, describing, sampling, constructing litho-graphic logs and checking the boundaries between the rock units of five representative outcrops covering the study area from south to north; Gebel El-Zeit, the Southern Galala, the Northern Galala, Gebel Ataqa and Gebel Shabraweet (Fig.1). 2). a total of about 850 rock samples were collected from these measured sections. 3). the vertical and lateral lithofacies changes of the exposed rocks were traced from the southern to the northern part of the study area. 4). the macrofossils encountered within the studied succession were identified in order to recognize the possible depositional environments of the Galala Formation. 5). more than three hundreds thin sections representing the different types of indurated rocks were selected, prepared and examined under the polarizing microscope for their composition, texture, macro- and microfaunal assemblage. Selected thin sections were stained with Alizarin Red-S and Potassium Ferricyanide following the method outlined by Dickson (1966), in order to differentiate between the carbonate minerals and to delineate the ferroan and non-ferroan dolomite. 6). twenty five samples were analyzed using the Scanning Electron Microscope (SEM) in order to elucidate their petrographic criteria and textural relationships.

FACIES ANALYSIS

Proximal or Inner Ramp Facies:

The inner ramp is the zone above fair-weather wave-base, where wave and current activities are almost continued (Reading 1996). The proximal inner ramp setting is typified by the coastal marine shoreface clastics to peritidal mixed clastic-carbonate facies of Gebel El-Zeit in the extreme southern part of the study area (Fig.2). The non-fossiliferous clastics (sandstone, siltstone, and claystones) form more than 50% of the total thickness of the Galala Formation exposed at Gebel El-Zeit. This environmental zone comprises two main dominant facies association that repeated vertically throughout the formation, the siliciclastic and mixed clastic-carbonate facies. A legend for the rock types, recognized constituents and sedimentary structures of the measured sections is given in Fig.3.

Siliciclastic-dominated facies:

The siliciclastic-dominated facies builds up the lowstand systems tracts (LSTs) of the Galala Formation at Gebel El-Zeit. Such facies indicates a lowering in sea level and hence suggests proximal inner ramp facies. It includes two types of facies; the coastal marine shoreface and the peritidal facies.

Coastal marine shoreface facies: This facies includes unfossiliferous coarse-grained sandstones in form of ferruginous, siliceous and dolomitic quartz arenites (Fig.4A-C). These sandstones are sometimes cross-laminated and most likely massive. The paucity of primary sedimentary structures and the absence of the biotic constituents, in addition to the coarse-grained texture point to shoreface environment as a transitional setting between the subaerial exposure and the shallow marine peritidal affinities (Olsen et al. 1999). The presence of cross-lamination in some layers indicates high energy shoreface environment (Nishikawa and Ito 2000). The scarcity of terrigenous mud is supportive of the nearshore coastal plain environment not far from land (Harris et al. 1997). The ferruginous, siliceous and dolomitic cements suggest deposition in a shallow nearshore environment with intermittent subaerial exposure (Khalifa and El-Ayyat 2007).

Peritidal facies: The Peritidal facies comprises supratidal swamp and marshes facies, supratidal-intertidal facies, and intertidal sand bars facies.

The supratidal swamp and marshes facies is mainly building up of fining-upward cycles at the uppermost part of Gebel El-Zeit. It consists of very shallow marine restricted siliciclastic sediments that are represented by calcareous and non-calcareous claystone, ferruginous quartz arenite and ferruginous sub-litharenite that are enriched in plant remains (Fig.4D). The lack of preserved marine biota and the absence of organic sedimentary structures (i.e. bioturbation) indicate a sheltered supratidal environment with a restricted circulation and elevated salinities (Elrick 1995). The plenty of plant remains reflects a vegetated swampy supratidal facies (Bauer et al. 2001 & 2003).

The supratidal-intertidal facies comprises the unfossiliferous claystone, glauconitic claystone, sandy glauconitic siltstone and flaser-, lenticular-bedded, inclined to vertical-burrowed sandstones with plant remains and wood stems (ferruginous, dolomitic, siliceous and evaporitic quartz arenites and glauconitic dolomitic litharenite) (Figs. 4E& F). The prevalence of quartz arenites characterizes the intertidal-supratidal settings of the inner ramp environment (Burchette and Wright 1992 and Schuzle et al. 2005). The sandy glauconitic siltstone and glauconitic sandstone indicate intertidal facies with normal salinity and slow rate of sedimentation (Genedi 1998 and El-Araby 2002). The vertical burrows characterize the intertidal substrate (Braithwaite and Talbot 1972 and Mansour et al. 2001). The rarity of carbonate fossils implies unfeasible ecological conditions for flourishing of organisms; such conditions prevail in high saline environment close to supratidal-intertidal affinities (Olsen et al. 1999). The accompaniment of the plant remains and the burrowing indicates that this facies was deposited in peritidal affinities with very shallow water depth close to the shore-beach realm. The occurrence of wood stems indicates a supratidal realm (Bauer et al. 2003). The presence of flaser and lenticular bedding suggests shallow intertidal sedimentation (Elrick and Read 1991). The clastic supratidal-intertidal facies of the present study is equivalent to the facies association-A of Wanas (2008) described from the Cenomanian of Sinai, Egypt.

The intertidal sand bars facies is represented by the planar cross-bedded and rippled sandstones that have been exposed in Gebel El-Zeit. Petrographic analysis indicates that the intertidal sand bars environment comprises one class of lithofacies; the ferruginous quartz arenite. The planar cross bedding in quartz arenite indicates high energy sedimentation on tidal bars (Khalifa and El-Ayyat 2007). The cross-bedded sandstones were interpreted to be deposited in intertidal suite (Elrick and Read 1991). The cross bedding and ripple marks sedimentary structures denote high energy intertidal sand bars (Blatt 1982). Similar facies were described and interpreted by Lüning et al. (1998a) and Mansour et al. (2001) to be belonged to the intertidal sand bar facies.

2-Mixed siliciclastic-carbonate facies:

The mixed siliciclastic-carbonate facies is represented by shallowing-upward cycles, each of which commences with green claystone and ends with sandy-ferroan dolomiticrite and dolosparite (Figs. 4G&H). Such type of cycles occurs in the transgressive systems tracts of Gebel El-Zeit, whereas the ferroan dolomiticrite forms the most cycle caps. Such facies indicates intertidal to supratidal settings, in which the Mg ions are available for dolomitization with association of iron oxides that came from the near hinterland. Dolostone exhibits an inner ramp setting (Read 1980 and Keller 1997). Burchette and Wright (1992) revealed that the dolomitization is the most prominent diagenetic feature on the shallow ramp.

Age	Rock Unit	Thickness (m)	Bed no.	Lithology	Lithologic characteristics	Litho-, microfacies	Depositional environments	Cycles
LATE CENOMANIAN TURKMAN	EL-KHASHIM FM		125		Dolostone, reddish yellow, very hard, fine-grained, form vertical walls, massive and bioturbated			
LATE CENOMANIAN TURKMAN	EL-KHASHIM FM	0.5	124	Ca - Ca	Sandstone, reddish brown, hard, fine-grained, with plant roots represents a paleosol horizon and with caliche nodules	Rooted ferruginous sub-litharenite	Supratidal swamps and marshes	S.B
		0.7	122	# # #				
		0.7	120	# # #	Four fining-upward cycles; based by reddish, fine-grained sandstone with plant remains and capped by dark grey, thin-laminated claystone enriched in plant remains	Ferruginous quartz arenite Claystone	Supratidal swamps and marshes	
		0.7	118	# # #				
		0.7	116	# # #				
		0.7	114	# # #				
		2.2	114	# # #	Sandstone, reddish brown, fine-grained, with selenitic gypsum layer and with plant remains	Rooted ferruginous sub-litharenite	Supratidal swamps and marshes	
		0.6	112	# # #				
		0.4	110	# # #	Claystone, grey, compact, calcareous and with plant remains	Claystone	Supratidal swamps and marshes	
		0.4	108	# # #				
		1.8	107	# # #	Three fining-upward cycles; based by cross-bedded sandstone and capped by soapy, sandy claystone	Sandy claystone Ferruginous quartz arenite	Supratidal-intertidal Intertidal sand bars	
		0.5	106	# # #				
		1.5	105	# # #	A coarsening-upward cycle; based by calcareous claystone with plant remains, and with geodes of limonitic concretions, followed by dolomitic, bioturbated sandstone and capped by ferruginous, gypsiferous sandstone with plant roots	Rooted ferruginous sub-litharenite Dolomitic quartz arenite Claystone	Supratidal swamps and marshes Supratidal-intertidal Supratidal swamps and marshes	
		0.8	-	# # #				
		0.5	-	# # #				
		0.8	-	# # #				
		0.5	-	# # #				
		0.5	-	# # #				
		3.0	97	# # #	Three alternating coarsening-upward cycles; based by grey, soapy, gypsiferous claystone and capped by cross-bedded sandstone	Ferruginous quartz arenite Claystone	Intertidal sand bars Supratidal-intertidal	
		1.5	96	Ca Ca Ca				
		1.0	95	Ca Ca Ca	Caliche, white, nodular, soft, freshwater zone and represents a sequence boundary	Recrystallized lime mudstone	Subaerial	S.B
		0.8	94	G G				
		0.8	93	G G	A coarsening-upward cycle; based by massive claystone with shell fragments and capped by ferruginated, dolomitic, burrowed sandstone	Dolomitic quartz arenite Claystone	Supratidal-intertidal Shallow subtidal	
		1.0	92	G G				
		0.5	91	G G	A coarsening-upward cycle; based by fissile claystone, middle by glauconitic, bioturbated sandstone and topped by bioturbated, dolomitic sandstone	Glauconitic dolomitic litharenite Claystone	Supratidal-intertidal	
		0.8	89	G G				
		0.5	88	G G	A shallowing-upward cycle based by calcareous claystone; followed by bioturbated sandstone and capped by sandy, glauconitic dolostone	Sandy glauconitic dolomitic Evaporitic quartz arenite Claystone	Supratidal-intertidal	
		4.3	87	G G				
2.0	76	G G	A coarsening-upward cycle; based by claystone and capped by bioturbated sandstone	Dolospirite Claystone	Supratidal-intertidal Shallow subtidal			
0.5	75	G G						
2.0	74	G G	Four alternating shallowing-upward cycles based by claystone with reworked oysters and capped by sandy, burrowed, glauconitic dolostone, bioturbated at the top	Ferroan dolomitic Evaporitic quartz arenite Claystone	Supratidal-intertidal Shallow subtidal			
1.7	73	G G						
1.0	58	G G	A shallowing-upward cycle; based by sandstone, with lenticular bedding and topped by sandy, burrowed dolostone	Ferruginous quartz arenite Claystone	Supratidal-intertidal			
1.0	57	G G						
1.0	56	G G	Four alternating coarsening-upward cycles based by semi-fissile claystone and capped by bioturbated, glauconitic sandstone	Ferruginous quartz arenite Claystone	Intertidal sand bars Supratidal-intertidal			
1.0	55	G G						
1.0	54	G G	Two alternating coarsening-upward cycles based by fissile claystone and capped by cross bedded sandstone	Fossiliferous marl Claystone	Restricted shallow marine Shallow subtidal			
1.0	53	G G						
1.0	52	G G	Two alternating cycles; based by claystone with reworked oysters and capped by massive and hard marls with reworked oysters	Glauconitic dolomitic litharenite Claystone	Supratidal-intertidal Shallow subtidal			
0.4	51	G G						
2.4	50	G G	A coarsening-upward cycle; based by claystone with reworked bivalves and topped by burrowed, dolomitic sandstone	Dolomitic marl Claystone	Supratidal-intertidal Shallow subtidal			
2.4	49	G G						
1.0	48	G G	A shallowing-upward cycle; based by massive claystone with reworked oysters and capped by bioturbated and dolomitic marl	Sandy dolomitic Siliceous quartz arenite	Supratidal-intertidal Coastal shoreface			
1.0	47	G G						
1.0	46	G G	Four alternating thin-based deepening-upward cycles; based by claystone with bivalves and capped by burrowed, sandy dolostone with reworked bivalves	Sandy dolomitic Siliceous quartz arenite	Supratidal-intertidal Coastal shoreface			
1.0	45	G G						
1.0	44	G G	A shallowing-upward cycle; based by fissile claystone, followed by hard sandstone shows flaser bedding with wood stems and topped by sandy dolostone, fossiliferous with oysters.	Sandy dolomitic Siliceous quartz arenite Claystone	Supratidal-intertidal			
1.8	43	G G						
6.0	42	G G	Five alternating coarsening-upward dwarf cycles; based by gypsiferous, massive claystone and capped by medium to coarse-grained sandstone	Siliceous quartz arenite Claystone	Coastal shoreface Supratidal-intertidal			
6.0	41	G G						
6.0	40	G G	Five alternating shallowing-upward cycles; based by calcareous claystone with reworked oysters and topped by burrowed, reddish yellow dolostone intensively bioturbated at the top	Ferroan dolomitic Claystone	Supratidal-intertidal Shallow subtidal			
6.0	39	G G						
1.0	22	G G	A shallowing-upward cycle; based by claystone, with gypsum veinlets and reworked oysters and capped by massive marl with reworked oysters	Fossiliferous marl Claystone	Restricted shallow marine Shallow subtidal			
3.4	21	G G						
0.6	15	G G	Three alternating shallowing-upward cycles; based by glauconitic claystone with reworked oysters and capped by burrowed dolostone	Ferroan dolomitic Glauconitic claystone	Supratidal-intertidal Shallow subtidal			
0.5	14	G G						
0.5	13	G G	Two shallowing-upward cycles; based by green claystone with reworked oysters and capped by burrowed dolostone with reworked oysters	Ferroan dolomitic Claystone	Supratidal-intertidal Shallow subtidal			
4.5	12	G G						
3.5	11	G G	Three alternating fining-upward cycles. Each cycle is based by burrowed sandstone with plant remains and capped by sandy siltstone with carbonized roots	Sandy glauconitic siltstone Ferruginous-dolomitic quartz arenite	Supratidal-intertidal			
3.5	10	G G						
0.9	9	G G	A deepening-upward cycle; based by green, sandy, siliceous claystone, that is overlain by cross-laminated sandstone and topped by massive, crystalline limestone	Lime mudstone Ferruginous quartz arenite Claystone	Restricted shallow marine Intertidal sand bars Supratidal-intertidal			
0.9	8	G G						
EARLY CRET.	MALHA FM		1		Dolostone, reddish brown, with plant roots a paleosol horizon, calcareous, sandy and with scattered rock fragments			

Fig.2: Vertical distribution of the lithologic characteristics, microfacies associations, depositional environments and depositional cycles of the Galala Formation at Gebel El-Zeit.

The mixed siliciclastic-carbonate inner ramp facies of the Galala Formation can be correlated with the shallow marine inner ramp facies of the Upper Albian-Cenomanian rocks of Areif El-Naqa area, northeast Sinai, Egypt (Lüning et al. 1998a).

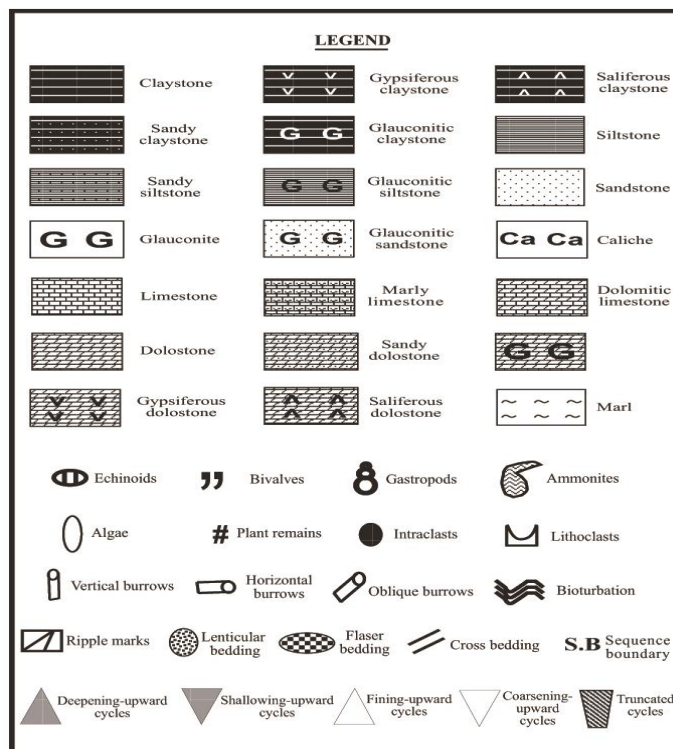


Fig.3: Legend for the rock types, recognized constituents, sedimentary structures and depositional cycles of the measured sections.

Middle ramp:

The mid ramp is the zone between the fair weather wave base and the storm wave base (Burchette and Wright 1992). This zone is characterized by the mixed siliciclastic-carbonate facies in the central part of the study area at the Southern and Northern Galalas and the carbonate-dominated facies in the northern part at Gebel Ataqa and Gebel Shabraweet (Figs. 5-8).

The lateral and vertical facies distribution on the mid ramp of the Galala Formation indicates that the ramp was drowned under influence of rapid pulses of local tectonic subsidence and maximally flooded in the central part of the study area forming a structural low (intra-ramp basin) at the Southern Galala. This structural low is most probably formed during the Triassic-Jurassic rifting process. Extension in most Mesozoic rift began at the end of the Permian, continued through the Triassic and the accelerated during the Jurassic in parallel with the opening of the western Tethys Ocean and the North Atlantic. This led to the development of north-northeast to northeast elongated rift basins on both sides of the Atlantic rifted zone (Guiraud et al. 2001). This opinion is contradicted with Kuss et al. (2000) as they considered the Galala Plateaus were affected by the Syrian Arc system. This is due to the absence of anticlinal structures that characterized the Syrian folding system. The Northern Galala exhibits shallower facies than the Southern Galala owing to the increment of dolostone. The gradual decrease in claystones and the spreading of the carbonate facies northwards indicates that the northern part of the study area has undergone a structural uplifting formed by the Syrian Arc System that results in evolution of a structural paleohigh (i.e. carbonate buildup) at Gebel Ataqa.

The cyclic sequence of the mid ramp of the Galala Formation comprises pure clastic, pure carbonate and hybrid clastic-carbonate shallowing-upward cycles. Such cyclic sequence elucidates that the period of the deposition of the Galala Formation is characterized by oscillation as evidenced by alternating shallower and deeper marine sediments. The mid ramp environment of the Galala Formation includes three facies types; the peritidal, shallow subtidal and deep subtidal.

1- Peritidal facies

Supratidal-shallow intertidal flat facies: It is the most common facies among the studied rocks. It is represented by the dolostones of the Southern and Northern Galalas, Gebel Ataqa and Gebel Shabraweet (mostly in the highstand systems tracts). These dolostones always cap the shallowing-upward cycles, which are based by low intertidal and subtidal facies. Two types of dolostone are present; the first and more abundant is the fine-crystalline dolostone (dolomicrite) (Fig.9A), while the second is the coarsely-crystalline dolostone (dolosparite) (Fig.9B). The fine-crystalline dolostones (dolomicrites) are originated during the early diagenetic events by the contemporaneous dolomitization of the precursor lime mud in the supratidal-shallow intertidal realm during a regressive phase (Al-Aasm and Packard 2000 and Lonnee and Al-Aasm 2000). The birdseyes (fenestral fabric) are detected within some dolomicrites (Fig.9C). Their presence suggests deposition in

peritidal environment (Shinn 1983). Similar facies was described from the "Dolomite Member" of the Abelgas Formation, Cantabrian Mountains, northern Spain by Keller (1997). The coarsely-grained dolostone (dolosparite) refers to late diagenetic dolomitization of the precursor dolomicrite in mixing meteoric-marine water during a progressive sea-level fall (Warren 2000).

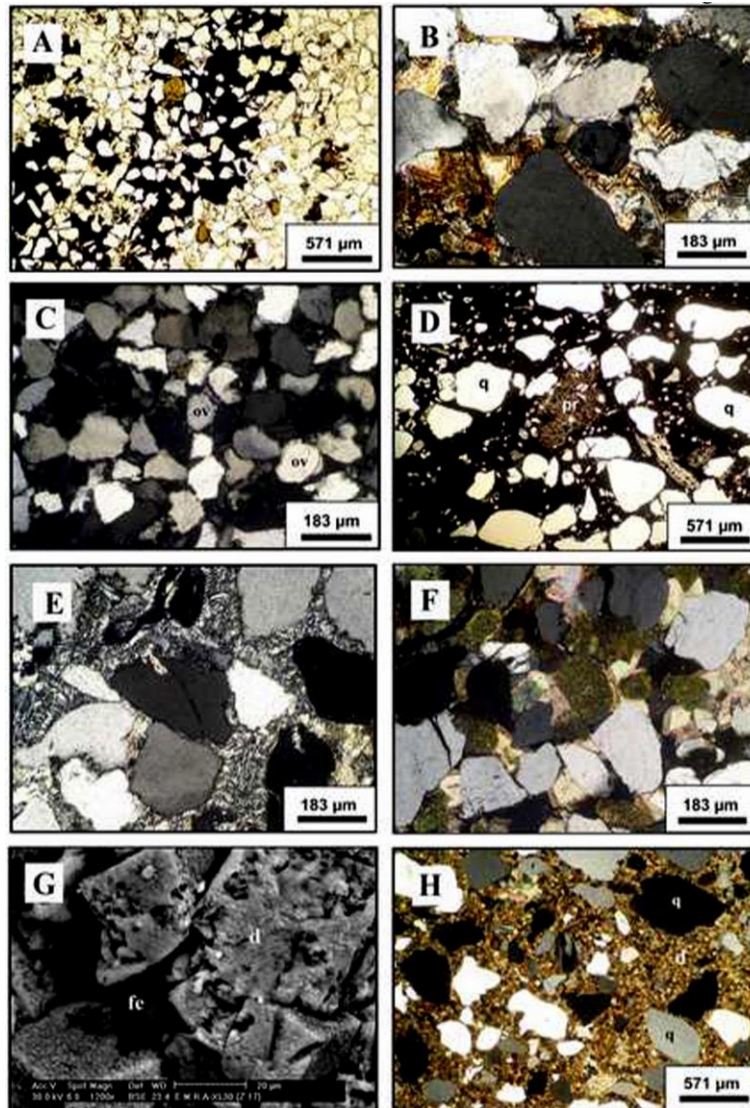


Fig. 4: **A.** Thin-section photomicrograph showing the ferruginous quartz arenite that consists of quartz grains cemented by iron oxide. Gebel El-Zeit. Ordinary light. **B.** Thin-section photomicrograph showing the dolomitic quartz arenite of the upper part of Gebel El-Zeit. Crossed polar light. **C.** Thin-section photomicrograph showing the siliceous quartz arenite. Notice: the silica overgrowth around the quartz grains (ov). Gebel El-Zeit. Crossed polar light. **D.** Thin-section photomicrograph showing the rooted ferruginous sub litharenite that is composed of quartz grains (q) and plant roots (pr) embedded in a ferruginous material. Gebel El-Zeit. Ordinary light. **E.** Thin-section photomicrograph showing the evaporitic quartz arenite that is composed of subrounded to subangular quartz grains cemented by fibrous evaporitic material. Gebel El-Zeit. Crossed polar light. **F.** Thin-section photomicrograph the glauconitic dolomitic litharenite lithofacies. It consists of quartz and glauconite grains cemented together by the planar, zoned dolomite cement. Gebel El-Zeit. Crossed polar light. **G.** SEM image showing a general picture of the ferroan dolomicrite lithofacies, in which the planar dolomites (d) are embedded in the ferruginous cement (fe) that shows black color. Gebel El-Zeit. **H.** Thin-section photomicrograph showing the sandy dolomicrite lithofacies. This lithofacies is composed of finely-crystalline, anhedral to subhedral dolomites (d) and quartz grains (q). Gebel El-Zeit. Crossed polar light.

Mid-deep intertidal flat facies: Mid-deep intertidal facies is represented by the dolomitic limestone facies. It includes the dolomitic lime mudstone of Gebel Ataqa and Gebel Shabraweet, dolomitic molluscan wackestone of the Northern Galala, Gebel Ataqa and Gebel Shabraweet (Fig.9D), dolomitic echinoidal wackestone of Gebel Shabraweet (Fig.9E) and the dolomitic algal bioclastic packstone of Gebel Ataqa (Fig.9F). Generally, the dolomitic limestone indicates an intertidal realm. The dolomitic lime mudstone is chiefly massive and bioturbated in few horizons. It is composed of dolomitic lime mud matrix with exceptional amount of shell debris, peloids, intraclasts, birdseyes and detrital quartz. The combination of the previous characteristics reflects deposition in a deep intertidal realm (El-Dawoody and Aboul Karamat 1993).

Age	Rock Unit	Thickness (m)	Bed no.	Lithology	Lithologic Characteristics	Litho-, micro facies	Depositional environments	Cycles			
L A T E C E N O M A N I A N	G A L A F O R M A T I O N		29		Limestone, grey, dolomitic with very large ammonites (ammonitic bed)						
			4.0	28		Limestone, nodular, cavernous, algal and fossiliferous with oysters	<i>Oncolitic packstone</i>		Shallow subtidal (restricted lagoon)		
			7.0	27		Claystone, forming oyster embankment	<i>Oyster claystone embankment</i> <i>Dol. peloidal packstone</i> <i>Oyster embankment</i>		Open marine shallow subtidal		
			1.0	26		Limestone, dolomitic, nodular with oysters	<i>Dol. algal bioclastic packstone</i>		Open marine shallow subtidal		
			1.0	25		Claystone, forming oyster embankment	<i>Oyster claystone</i>		Open marine shallow subtidal		
			1.0	24		Limestone, dolomitic with oysters and echinoderms	<i>Dol. algal bioclastic packstone</i>		Open marine shallow subtidal		
			1.0	23		Claystone, yellowish green, soft and rich in oysters	<i>Oyster claystone</i>		Open marine shallow subtidal		
			1.0	22		Limestone, dolomitic with oysters and echinoderms	<i>Dol. algal bioclastic packstone</i>		Open marine shallow subtidal		
			2.0	21		Claystone, yellowish green, soft and rich in oysters	<i>Oyster claystone</i>		Open marine shallow subtidal		
			0.8	20			<i>Bioclastic foraminiferal wackestone</i>				
			13.5	19		A shallowing-upward cycle; based by gypsiferous claystone with ammonites and echinoderms and rich in oysters forming oyster embankment and capped by marly, massive limestone, fossiliferous with oysters and echinoderms	<i>Oyster claystone embankment</i>		Open marine shallow subtidal		
			0.6	18			<i>Bioclastic foraminiferal wackestone</i>		Open marine shallow subtidal		
			0.5	17			<i>Oyster claystone embankment</i>		Open marine shallow subtidal		
			0.6	16		Limestone, grey to pale yellow, massive and enriched in oysters and ammonites	<i>Bioclastic foraminiferal wackestone</i>		Open marine shallow subtidal		
			16.0	15		Claystone, yellowish green, soft, gypsiferous glauconitic, sandy, massive, with ammonites and enriched in oysters forming oyster embankment	<i>Oyster claystone embankment</i>		Open marine shallow subtidal		
			0.6	14		Limestone, massive, fossiliferous and enriched in oysters and ammonites	<i>Bioclastic foraminiferal wackestone</i>		Open marine shallow subtidal		
			7.0	13		Claystone, yellowish green, soft, massive, gypsiferous, glauconitic, sandy and rich in oysters forming oyster embankment	<i>Oyster claystone embankment</i>		Supratidal-shallow intertidal		
			0.6	12		Dolostone, yellowish red, massive, fine-grained, sandy, glauconitic and with oyster fragments	<i>Ferroat dolomicrite</i>		Supratidal-shallow intertidal		
			2.5	11		Claystone, gypsiferous, glauconitic, sandy and rich in oysters forming oyster embankment	<i>Oyster claystone embankment</i>		Open marine shallow subtidal		
			1.0	10		Sandstone, glauconitic, cross-bedded and ferruginous	<i>Sandy dolomitic glauco-arenite</i> <i>Ferruginous Qz arenite</i>		Deep subtidal		
			0.4	9			<i>Ferruginous Qz arenite</i>		Intertidal sand bar		
			1.7	8		Claystone, gypsiferous and rich in oysters	<i>Oyster claystone</i>		Open marine shallow subtidal		
			3.5	6		A shallowing-upward cycle; based by gypsiferous claystone with bivalves and capped by medium-grained, ferruginous sandstone, with ripple marks	<i>Ferruginous Qz arenite</i> <i>Oyster claystone</i>		Intertidal sand bar Open marine shallow subtidal		
			0.4	5		A shallowing-upward cycle; based by gypsiferous claystone enriched in oysters and capped by massive to cross-bedded, medium-grained lithoclastic sandstone	<i>Ferruginous Qz arenite</i> <i>Oyster claystone</i>		Intertidal sand bar Open marine shallow subtidal		
			3.5	4		A shallowing-upward cycle; based by claystone with oysters and capped by cross-bedded sandstone with medium to very coarse-grained	<i>Ferruginous Qz arenite</i> <i>Oyster claystone</i>		Intertidal sand bar Open marine shallow subtidal		
			0.6	3			<i>Ferruginous Qz arenite</i>		Intertidal sand bar		
			1.7	2			<i>Oyster claystone</i>		Open marine shallow subtidal		
			EARLY CRET.	MALHA FM.		1			Sandstone, reddish brown, coarse-grained, above this bed there is a red crust (paleosol)		

Fig.5: Vertical distribution of the lithologic characteristics, microfacies associations, depositional environments and depositional cycles of the Galala Formation at the Southern Galala.

Age	Rock Unit	Thick. (m)	Bed no.	Lithology	Lithologic characteristics	Litho-, micro facies	Depositional environments	Cycles
L A T E C R E T A C E O U S L A T E C R E T A C E O U S L A T E C R E T A C E O U S L A T E C R E T A C E O U S	MALHA FM.	4m 3m 2m 1m	84		Dolostone, fine-grained, forming vertical wall, jointed, cracked			
			1.0	83	Claystone, gypsiferous (base of truncated cycle) capped by white caliche zone (subaerial exposing)	Claystone	Restricted lagoon	
			1.0	82	A shallowing-upward cycle; based by claystone, fissile, nodular with bivalves and topped by marly, massive dolomitic limestone	Ostracod molluscan packstone Oyster claystone	Open marine shallow subtidal	
			2.5	81	A shallowing-upward cycle; based by claystone, fissile, nodular with oysters and topped by hard, massive dolostone with bivalves fragments	Dolomicrite Oyster claystone	Supratidal-shallow intertidal Open marine shallow subtidal	
			0.5	80	A shallowing-upward cycle; based by claystone, fissile, nodular with oysters and topped by hard, massive dolostone with bivalves fragments	Ostracod molluscan packstone Oyster claystone	Open marine shallow subtidal	
			1.0	78	A shallowing-upward cycle; based by claystone, fissile, nodular with oysters and topped by marly, molluscan limestone	Ostracod molluscan packstone Oyster claystone	Open marine shallow subtidal	
			3.0	77	Two shallowing-upward cycles; based by massive claystone with bivalves and capped with nodular, dolomitic limestone with bivalves	Ostracod molluscan packstone Oyster claystone	Open marine shallow subtidal	
			1.0	76	Four alternating shallowing-upward cycles; based by nodular, calcareous claystone forming oyster embankment and topped by massive, hard limestone with bivalvia and echinoderms	Foraminiferal molluscan packstone Bioclastic foraminiferal wackestone Claystone embankment	Open marine shallow subtidal	
			2.5	75	A shallowing-upward cycle; based by claystone forming oyster embankment and capped with hard limestone forming oyster embankment	Foram. molluscan packstone Claystone embankment	Open marine shallow subtidal	
			1.0	74	Two shallowing-upward cycles; based by claystone forming oyster embankment and topped by massive, crystalline limestone with oysters	Bioclastic foraminiferal wackestone Claystone embankment	Open marine shallow subtidal	
			1.0	73	Three alternating shallowing-upward cycles; each is based by gypsiferous and saliferous claystone and capped by thick-bedded dolostone	Dolomicrite Claystone	Supratidal-shallow intertidal Shallow subtidal	
			0.6	72	A shallowing-upward cycle; based by saliferous and friable claystone and capped with burrowed dolostone	Dolomicrite	Supratidal-shallow intertidal	
			1.0	71	Three alternating shallowing-upward cycles; each is based by white, marly limestone with scarce fossils and capped by burrowed dolostone	Lime mustone Dolomicrite	Shallow subtidal (lagoon) Supratidal-shallow intertidal	
			1.0	70	A shallowing-upward cycle; based by claystone, fissile with gypsum layers and capped with dolostone, grey, gypsiferous and fractured	Dolomicrite Claystone	Supratidal-shallow intertidal Shallow subtidal	
			0.5	69	Two shallowing-upward cycles; based by fissile claystone and capped by prous, molluscan dolomitic limestone	Dol. molluscan wackestone Claystone	Mid-deep intertidal Shallow subtidal	
			1.0	68	Limestone, porous, dolomitic and molluscs	Dol. molluscan wackestone Fossiliferous marl	Mid-deep intertidal Shallow subtidal (restricted lagoon)	
			0.5	67	Three deepening-upward cycles; each is based by siltstone, sandy and glauconitic and capped with marls, with bivalves	Sandy glauconitic siltstone Bioclastic foraminiferal wackestone	Supratidal-intertidal Open marine shallow subtidal	
			1.0	66	A shallowing-upward cycle based by glauconitic claystone forming oyster embankment and capped by nodular, marly limestone with bivalves and echinoderms	Oyster claystone embankment Fossiliferous marl Oyster claystone	Shallow subtidal (lagoon) Open marine shallow subtidal	
			0.5	65	Marl, massive and fossiliferous with bivalves	Fossiliferous marl	Shallow subtidal (restricted lagoon)	
			1.0	64	Claystone, friable and fossiliferous with oysters and echinoderms forming oyster embankment	Oyster claystone embankment	Open marine shallow subtidal	
			0.5	63	Marl, creamy white, hard, massive and fossiliferous with oysters	Oyster claystone embankment	Open marine shallow subtidal	
			1.0	62	Claystone, reddish green, gypsiferous, saliferous, massive and fossiliferous with oysters and echinoderms forming oyster embankment	Dolomicrite Claystone	Supratidal-shallow intertidal Shallow subtidal	
			0.5	61	Three alternating shallowing-upward cycles; each is based by gypsiferous and calcareous claystone and capped by dolostone, sandy, glauconitic, with reworked oysters and burrowed at the top	Dolomicrite	Supratidal-shallow intertidal	
			1.0	60	Six alternating shallowing-upward cycles; each is based by gypsiferous, saliferous claystone and capped by burrowed dolostone	Dolomicrite Claystone	Supratidal-shallow intertidal Shallow subtidal	
			3.0	59	A shallowing-upward cycle; based by oyster claystone, that is overlain by sandy dolostone and capped by reddish pink, ledge-forming dolostone	Sandy-dolomicrite Oyster claystone	Supratidal-shallow intertidal Open marine shallow subtidal	
			2.5	A shallowing-upward cycle, based by gypsiferous claystone with oysters, that is overlain by laminated, glauconitic siltstone and capped by sandy, massive dolostone	Sandy dolomicrite Sandy glauconitic siltstone Oyster claystone	Supratidal-shallow intertidal Supratidal-intertidal Open marine shallow subtidal	
			1.0	52				
			1.5	51				
			4.0				
			0.5	44				
			0.9	43				
			0.5	42				
			1.7	41				
			0.5	40				
0.5	39							
0.5	38							
0.5	37							
0.8	36							
0.5	35							
0.8	34							
0.5	33							
0.8	32							
1.5	31							
2.0	30							
1.0	29							
0.9	28							
2.5	27							
6.0	26							
2.7							
5.2							
0.7	7							
0.5	6							
0.8	5							
0.5	4							
2.0	2							
	1							

Fig.6: Vertical distribution of the lithologic characteristics, microfacies associations, depositional environments and depositional cycles of the Galala Formation at the Northern Galala.

Age	Rock Units	Thickness (M)	Bed no.	Lithology	Lithologic characteristics	Litho-, micro facies	Depositional environments	Cycles	
L A T E C R E T A C E O U S L A T E C E N O M A N I A N G A L A F O R M A T I O N	KL-KHASHM FM.	1.3	77		Dolomite, fine-grained, forming vertical wall, jointed	<i>Dolomitic lithoclastic lime mudstone</i>	Mid-deep intertidal flat	▼	
		1.5	76		Limestone, marly and massive	<i>Lime mudstone</i>	Restricted lagoon		
		0.5	75		A shallowing-upward cycle; based by marly limestone and capped by massive dolomitic limestone	<i>Dolomitic lime mudstone</i>	Mid-deep intertidal flat		
		1.0	74		A shallowing-upward cycle; based by thin-laminated, bioturbated limestone and capped by grey, burrowed dolomite with oyster fragments	<i>Lime mudstone</i>	Restricted lagoon		
		2.0	73		A shallowing-upward cycle; based by marly and fractured limestone and capped by massive and dolomitic limestone	<i>Dolomitic lime mudstone</i>	Mid-deep intertidal flat		
		2.5	72			<i>Lime mudstone</i>	Restricted lagoon		
		0.5	71						
		5.0	70						
		0.4	69						
		1.5	68						
		0.4	67						
		1.5	66						
		0.4	65						
		1.5	64						
		2.0	63						
		1.5	62						
		2.5	61						
		0.3	60						
		7.5	59						
		3.0	58						
		0.6	57						
		0.3	56						
		0.5	55						
		0.3	54						
		1.8	49						
		0.5	48						
		4.0	46						
		0.6	45						
		0.3	44						
		0.4	43						
		0.4	42						
		12.0							
		2.0	29						
		0.5	28						
		7.2							
		9.0							
		1.5	13						
		2.0	12						
		1.5	11						
		0.5	10						
0.4	9								
0.7	8								
0.4	7								
0.5	6								
1.3	5								
0.7	4								
0.4	3								
1.5	2								
0.4	1								

Fig.7: Vertical distribution of the lithologic characteristics, microfacies associations, depositional environments and depositional cycles of the Galala Formation at Gebel Ataqa.

Age	Rock Units	Thickness (m)	Bed no.	Lithology	Lithologic characteristics	Litho-, micro facies	Depositional environments	Cycles		
L A T E C R E T A C E O U S	L A T E C R E T A C E O U S	4m 3m 2m 1m	42			A shallowing-upward cycle; based by hard, massive and fine-grained dolostone and capped by hard, massive, crystalline, highly bioturbated, nodular, burrowed, thin-laminated dolostone with calcite vugs	<i>Dolosparite</i>	Supratidal-shallow intertidal	Cycles	
			41					<i>Dolomicrite</i>		Supratidal-shallow intertidal
			40			A shallowing-upward cycle; based by massive claystone forming oyster embankment, middled by massive, fine-grained dolostone that is bioturbated at the top and capped by cavernous, gypsiferous, burrowed, massive and coarse-grained dolostone	<i>Dolosparite</i>	Supratidal-shallow intertidal		
			39	42.4				<i>Dolomicrite</i>		Supratidal-shallow intertidal
			38					<i>Oyster claystone embankment</i>		Open marine shallow subtidal
			37				A shallowing-upward cycle; based by massive claystone forming oyster embankment and capped by thin-laminated, burrowed dolostone with mud cracks at the top	<i>Dolosparite</i>		Supratidal-shallow intertidal
			36					<i>Oyster claystone embankment</i>		Open marine shallow subtidal
			35				Two shallowing-upward cycles; each is based by massive claystone forming oyster embankments and capped by massive to thin-laminated, fossiliferous limestone with bivalves and echinoderms	<i>Peloidal echinoidal grainstone</i>		Restricted shoal
			34	9.6				<i>Oyster claystone embankment</i>		Open marine shallow subtidal
			33					<i>Oolitic peloidal grainstone</i>		Restricted shoal
32					<i>Oyster claystone embankment</i>	Open marine shallow subtidal				
31					<i>Dolomicrite</i>	Supratidal-shallow intertidal				
30	2.8			A shallowing-upward cycle; based by burrowed, fossiliferous limestone and capped by hard, massive and fine-grained dolostone	<i>Molluscan peloidal packstone</i>	Restricted lagoon				
29					<i>Dol. echinoidal wackestone</i>	Mid-deep intertidal				
28					<i>Oyster claystone</i>	Open marine shallow subtidal				
27	5.2			Three shallowing-upward cycles. The first is based by cavernous dolomitic limestone and capped by massive dolostone with gypsum veinlets. The second and third are based by calcareous claystone, fossiliferous with oysters and capped by thin-laminated dolostone and fossiliferous dolomitic limestone respectively	<i>Dolomicrite</i>	Supratidal-shallow intertidal				
26					<i>Oyster claystone</i>	Open marine shallow subtidal				
25					<i>Dolomicrite</i>	Supratidal-shallow intertidal				
24					<i>Dolomitic lime mudstone</i>	Mid-deep intertidal				
23					<i>Dol. echinoidal wackestone</i>	Mid-deep intertidal				
22	4.2			Two shallowing-upward cycles; the first is based by fissile claystone, fossiliferous with oysters and topped by burrowed, crystalline limestone and the second is based by green claystone forming oyster embankment and capped by cavernous, fossiliferous dolomitic limestone	<i>Oyster claystone</i>	Open marine shallow subtidal				
21					<i>Molluscan peloidal packstone</i>	Restricted lagoon				
20					<i>Oyster claystone</i>	Open marine shallow subtidal				
19					<i>Dolomicrite</i>	Supratidal-shallow intertidal				
18	9.0			Repetitive shallowing-upward cycles; based by greenish claystone, forming oyster embankment, calcareous, fissile in some beds and capped by oyster limestone embankment or by fractured, burrowed and massive dolostone	<i>Oyster claystone</i>	Open marine shallow subtidal				
17					<i>Mollusc-echin. wackestone</i>	Open marine shallow subtidal				
16					<i>Oyster claystone embankment</i>	Open marine shallow subtidal				
15					<i>Dolomicrite</i>	Supratidal-shallow intertidal				
14					<i>Oyster claystone embankment</i>	Open marine shallow subtidal				
13	3.0			A shallowing-upward cycle; based by massive limestone forming oyster embankment and capped by massive and molluscan dolostone	<i>Dolomicrite</i>	Supratidal-shallow intertidal				
12					<i>Mollusc-echin. wackestone</i>	Open marine shallow subtidal				
11				Sandstone, hard and ferruginous						

Fig.8: Vertical distribution of the lithologic characteristics, microfacies associations, depositional environments and depositional cycles of the Galala Formation at Gebel Shabraweet.

Age	Rock Units	Thickness (m)	Bed no.	Lithology	Lithologic characteristics	Litho-, micro facies	Depositional environments	Cycles		
									Tur.-Sant.	
L A T E C E N O M A N I A N S	M a g h r a E l - H a d i d a F m.	4m 3m 2m 1m				Limestone, white, marly, hard and massive				
			119					<i>Siliceous ferruginous dolomicrite</i>	Subaerial	▲
			118	8.7		A shallowing-upward cycles; based by thick-bedded dolomitic limestone, overlaid by massive, burrowed, fine-grained dolostone, that is overlaid by burrowed, porous, coarse-grained dolostone and capped by dark brown, cherty, ferruginated dolostone	<i>Dolosparite</i>	Supratidal-shallow intertidal		
			117				<i>Dolomicrite</i>	Supratidal-shallow intertidal		
			116				<i>Dolomitic lime mudstone</i>	Mid-deep intertidal		
			115	9.0		Three shallowing-upward cycles; each is based by marly, massive limestone and capped by massive, burrowed dolostone, while the second one is middled by thick-bedded dolomitic limestone	<i>Dolomicrite</i>	Supratidal-shallow intertidal	▲	
			108				<i>Dolomitic lime mudstone</i>	Mid-deep intertidal		
			107				<i>Lime mudstone</i>	Restricted lagoon		
			106	9.5		A shallowing-upward cycle; based by marly, massive limestone, middled by thick-bedded dolomitic limestone and capped by thin-laminated, fractured dolostone	<i>Dolosparite</i>	Supratidal-shallow intertidal	▲	
			105				<i>Dolomitic lime mudstone</i>	Mid-deep intertidal		
			104				<i>Lime mudstone</i>	Restricted lagoon		
			103	4.0		A shallowing-upward cycle; based by marly, burrowed limestone and topped by highly-bioturbated, thin-laminated dolostone	<i>Dolomicrite</i>	Supratidal-shallow intertidal	▲	
			102				<i>Lime mudstone</i>	Restricted lagoon		
			101	10.0		A shallowing-upward cycle; based by oyster claystone embankment, overlaid by marly, massive and highly fossiliferous limestone, that is overlaid by massive, fine-grained dolostone and capped by grey, massive, coarse-grained dolostone	<i>Dolosparite</i>	Supratidal-shallow intertidal	▲	
			100				<i>Dolomicrite</i>	Supratidal-shallow intertidal		
			99				<i>Molluscan-echinoidal wackestone</i>	Open marine shallow subtidal		
			98	11.0		Three shallowing-upward cycles; based by marly, fractured limestone and capped by partially crystalline, porous, fractured dolostone	<i>Oyster claystone embankment</i>	Open marine shallow subtidal	▲	
			97				<i>Dolomicrite</i>	Supratidal-shallow intertidal		
			96				<i>Lime mudstone</i>	Restricted lagoon		
			95	13		Glauconite, deep green, white limestone nodules and fossiliferous with oysters Claystone, green, glauconitic and fossiliferous with oysters	<i>Sandy dolomitic glauco-arenite</i>	Deep subtidal	▲	
			94				<i>Oyster claystone</i>	Open marine shallow subtidal		
			93				Five repetitive shallowing-upward cycles; based by green, calcareous, nodular claystone, fossiliferous with oysters and capped by hard, white, sandy limestone, fossiliferous with echinoderms and molluscs	<i>Molluscan-echinoidal wackestone</i>		Open marine shallow subtidal
			92	9.6		Repetitive shallowing-upward cycles; based by green, calcareous, nodular claystone, fossiliferous with oysters and capped by hard, massive, marly dolomitic limestone or by marly, molluscan dolomitic limestone	<i>Oyster claystone</i>	Open marine shallow subtidal	▲	
			91				<i>Dol. molluscan wackestone</i>	Mid-deep intertidal		
90			<i>Oyster claystone</i>		Open marine shallow subtidal					
89	15.5		Repetitive shallowing-upward cycles; based by green, calcareous, massive, nodular claystone, fossiliferous with oysters and capped by hard, massive dolomitic limestone	<i>Dolomitic lime mudstone</i>	Mid-deep intertidal	▲				
88				<i>Oyster claystone</i>	Open marine shallow subtidal					
87				<i>Dolomitic lime mudstone</i>	Mid-deep intertidal					
86	6.6		A shallowing-upward cycle; based by fractured dolomitic limestone, middled by sandy, bioturbated dolostone and capped by burrowed and crystalline dolostone	<i>Oyster claystone</i>	Open marine shallow subtidal	▲				
85				<i>Dolomicrite</i>	Supratidal-shallow intertidal					
84				<i>Sandy dolomicrite</i>	Supratidal-shallow intertidal					
83				<i>Dolomitic lime mudstone</i>	Mid-deep intertidal					

Fig.8 Continuous

The allochems of the dolomitic wackestone and packstone are mostly dolomitized oysters, echinoderms with subordinate amount of ostracod shells, dasycladacean green algae, peloids, ooids and intraclasts. The presence of massive dolomitic wackestone and packstone enriched in diversified allochems implies open marine mid-deep intertidal flat facies with low energetic conditions (Lüning et al. 1998b). Similar facies was identified from the low-mid intertidal flat of the Cenomanian Halal Formation of Gebel Halal, north Sinai, Egypt by El-Araby (2002).

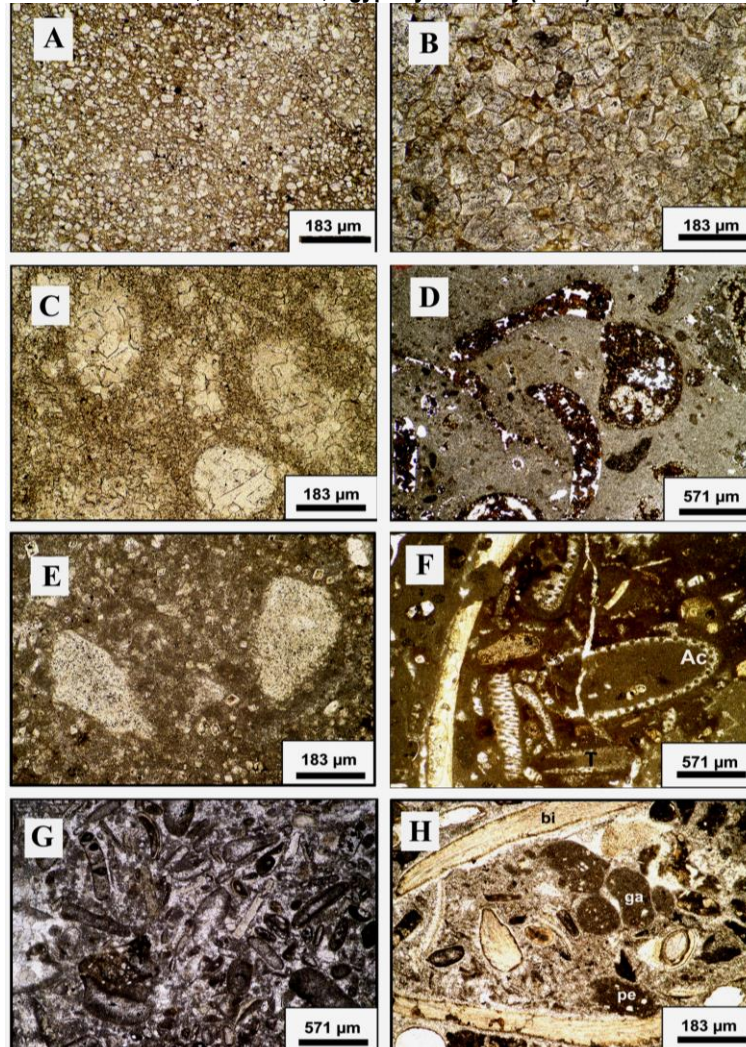


Fig. 9: **A.** Thin-section photomicrograph showing the dolomitic lithofacies. The rock is composed of euhedral dolomitic rhombs embedded in a microcrystalline calcitic matrix. The Northern Galala. Ordinary light. **B.** Thin-section photomicrograph showing hypidiotopic to idiotopic dolomites with cloudy centers, forming the dolosparite lithofacies. Gebel Ataqa. Ordinary light. **C.** Thin-section photomicrograph showing the birdseye dolomitic. Notice: the elliptical, lensoidal or rounded birdseyes structures are filled with calcite and walled by dolomite rhombs. Gebel Ataqa. Ordinary light. **D.** Thin-section photomicrograph showing the dolomitic molluscan wackestone, in which the molluscan particles (bivalves and gastropods) have been replaced by planar, ferroan dolomite rhombs. These allochems are embedded in a micritic matrix. The Northern Galala. Ordinary light. **E.** Thin-section photomicrograph showing dolomitic echinoidal wackestone. Notice: the hypidiotopic to idiotopic, zoned dolomite rhombs replace both the matrix and the echinodermdal fragments. Gebel Shabraweet. Ordinary light. **F.** Thin-section photomicrograph showing the dolomitic algal bioclastic packstone. It is made up of oyster, echinodermal and algal fragments. The algal particles are represented by *Trinocladus tripoliatus* Raineri (T) and *Acroporella* sp. (Ac). Gebel Ataqa. Ordinary light. **G.** Thin-section photomicrograph showing the oncolitic packstone. The allochems are formed of algal oncolites, bioclasts and peloids embedded in a lime mud. The Southern Galala. Ordinary light. **H.** Thin-section photomicrograph showing the molluscan peloidal packstone. The particles are mainly formed of bivalvian (bi) and gastropods (ga) besides the peloids (pe) and shell debris embedded in a micritic matrix. Gebel Shabraweet. Ordinary light.

2- Shallow subtidal facies:

Restricted lagoonal facies: The protected lagoonal facies of the Galala Formation is represented by the fossiliferous marl, lime mudstone, oncolitic packstone and the molluscan peloidal packstone. The presence of the micritic matrix indicates that the wave and current action were not strong enough to hinder the accumulation of micrite, therefore it reflects deposition in a restricted lagoonal environment.

The fossiliferous marl is recognized from several levels at the middle parts of the Northern Galala and Gebel Ataqa. These marls are massive and enriched in molluscs. The lime mudstone is considered as the most common widely

distributed lagoonal subtidal facies. It is repeated vertically throughout Gebel Ataqa and Gebel Shabraweet (transgressive and highstand systems tracts). Also, it was identified from few beds near the middle part of the Northern Galala. It mostly exhibits no sedimentary structures. The oncolitic packstone is confined to one bed at the uppermost part of the Southern Galala, at which the allochems are dominated by algal oncoids, pelecypods, green algae, ostracods, miliolids and peloids (Fig.9G). The molluscan peloidal packstone occurs at the lower part of Gebel Shabraweet, whereas the rock is bioturbated with horizontal burrows. The bulk of this rock is made up of peloids, molluscs, echinoids, green algae, ostracods and miliolids (Fig.9H). The fossiliferous marls indicate deposition in low energy restricted shallow marine environment (Bauer et al. 2003). The massive nature of these rocks designates shallow marine restricted conditions. The homogeneous, scarcely fossiliferous, non-laminated lime mudstone accumulates in a restricted shallow subtidal marine environment of high salinity, probably lagoon (Sanders and Höfling 2000). It is corresponding to the standard microfacies association SMF-23 of Wilson (1975) and MFT-4a of Lakew (1990). The oncolitic-algal-miliolidae-ostracodal-peloidal facies points to lagoonal environments (Enos 1983; Kuss and Malchus 1989 and Bauer et al. 2002). The low-energy lagoonal environments are dominated by the green algae (Wray 1977).

The existence of ostracods is an indicator about a restricted shallow subtidal environment (Aurell 1991). The oncolitic packstone facies association is equivalent to SMF-22 of Wilson (1975). The lagoonal facies includes bioclastic, peloidal packstones that dominated with miliolids, calcareous algae, gastropods, ostracods and micrite cement (Pomar 2001 and Khalifa et al. 2004). The peloidal facies is common in the quiet, shallow marine restricted lagoonal environment with slow sedimentation (Tucker and Wright 1990 and Evans et al. 1995). Such facies is consistent with SMF-19 of Wilson (1975).

Restricted shoal facies: The restricted shallow subtidal shoal facies of the Galala Formation includes two microfacies; the peloidal echinoidal and oolitic peloidal grainstones. They are building up two thin beds at the lower part of Gebel Shabraweet. Petrographically, the rock is composed of allochemical constituents embedded in sparry calcite cement. The allochemical components are composed mainly of peloids, oolites, echinoids, molluscs, miliolids, intraclasts, bryozoa and ostracoda (Fig.10A). The restricted shoals are developed within the mid ramp setting (Bádenas and Aurell 2001 and Puga-Bernabéu et al. 2007). The bioclastic-oolitic-peloidal grainstone of the studied facies is interpreted to represent a submarine patchy carbonate shoals locally developed in a high energy, shallow subtidal regime of an interior shelf lagoon along its landward area. During the re-deposition in the shoals, the reworked particles (skeletal grains and peloids) were surrounded by the superficial ooid coatings (Lüning et al. 1998a). The skeletal oolitic-peloidal grainstone facies is deposited in current or wave-agitated shallow subtidal environments (Wilkinson et al. 1997). The oolitic-peloidal-intraclastic grainstone is deposited in agitated, shallow subtidal water as low-relief shoal (i.e. restricted shoal) (Tucker et al. 1993, Lüning et al. 1998b and Hofmann et al. 2004). The high diversity of allochems (echinoids, bryozoa, mollusca, peloids, ooids and intraclasts) embedded in a sparry calcite cement points to an influence of shallower and more agitated water, probably shoal area (Wilson 1975 and Flugel 1982). Such grainstones are equivalent to SMF-16 of Wilson (1975).

Open marine shallow subtidal facies:

The open marine shallow subtidal facies is characterized by highly diverse fossil assemblages. It is represented by the fossiliferous claystone, limestone and dolomitic limestone. The open marine shallow subtidal green claystones are recognized from the Southern and Northern Galalas, Gebel Ataqa and Gebel Shabraweet, where they build up the base of the shallowing-upward cycles. They are dominated by bivalves (mainly oysters), gastropods and echinoderms. The ammonites are distinguished only from the Southern Galala. The open marine shallow subtidal limestones are represented by the molluscan-echinoidal wackestone, bioclastic foraminiferal wackestone, foraminiferal molluscan packstone and ostracoda molluscan packstone (Figs.10B-D). The molluscan-echinoidal wackestone is recorded only from Gebel Shabraweet, whereas they are made up of micritic matrix, skeletal components (oysters, echinoids, ostracods, gastropods, large foraminiferal grains and phosphatic bone fragments) and glauconite pellets. The bioclastic-planktonic foraminiferal-molluscan wackestones and packstones are distinguished from the Northern and Southern Galalas. The dolomitic limestones of the open marine shallow subtidal comprise the dolomitic algal bioclastic packstone and dolomitic peloidal packstone that were recognized from the Southern Galala (Figs.10E&F).

The presence of claystones and limestones enriched in different varieties of fossils suggests deposition in an open marine shallow subtidal environment with normal salinity (Gawthorpe 1986). The green claystones that contain megafossils (molluscs and echinoids) indicate a shallow subtidal environment (Khalifa and Kandil 2004) with deeper conditions at the Southern Galala due to the presence of ammonites. The occurrence of echinoids and oysters in a micritic matrix reflects a well-oxygenated, normal saline, open marine shallow subtidal environment (Lakew 1990). Consequently, these mud-supported rocks denote a shallow subtidal environment with open circulation comparable to SMF-9 of Wilson (1975). The presence of nektonplanktonic ammonites (e.g. *Neolobites*) points to the interfingering of foreigner deeper ramp sediments with the dominated shallower marine deposits under the effect of wave action and high energetic currents (Bauer et al. 2001). The presence of the globular planktonic forams (heterohelicid and hedbergellid) with absence of the keeled forams in the Northern and Southern Galalas suggest a shallow ramp environment (Grosheiny and Malartre 2002). The lack of deeper marine rotaloporids in the Cenomanian rocks of the north Eastern Desert refers to a deep shallow subtidal environment with depth ranging from 50-100 m and open circulation (Ismail and Akarish 2000 and Kora et al. 2001b). Similar mid ramp facies was given by Youssef et al. (2002) to interpret the Late Paleocene-Early Eocene succession of the Southern Galala. They attributed the occurrence of the deeper marine fauna (e.g. planktonic foraminifera) within the

shallow ramp facies to the flooding periods during the deposition of their studied sequence. The high diversity of dolomitized allochems (oysters, echinoids, planktonic foraminifera, ostracods, green algae, algal oncolites and peloids) embedded in a micritic matrix indicates an open shallow marine environment with turbulence during deposition. These associations are equivalent to MFT-8 of Schulze et al. (2005).

Oyster embankment facies: The oyster embankment facies is typified by the piling up of large-sized oyster shell fragments in claystones and limestones. The lack of such embankments in Gebel El-Zeit is probably owed to high rates of clastic influx that exceed the biogenic accumulation and presence of relatively restricted conditions due to tightness of the depositional basin at Gebel El-Zeit. The oyster claystone embankments are recognized from the Southern and Northern Galalas and Gebel Shabraweet. These claystones are loaded with oyster debris (> 60%) and also enclose skeletal particles of echinoids, planktonic foraminifera, ostracods and ammonites in few horizons. The oyster limestone embankments are identified from the upper part of the Northern Galala.

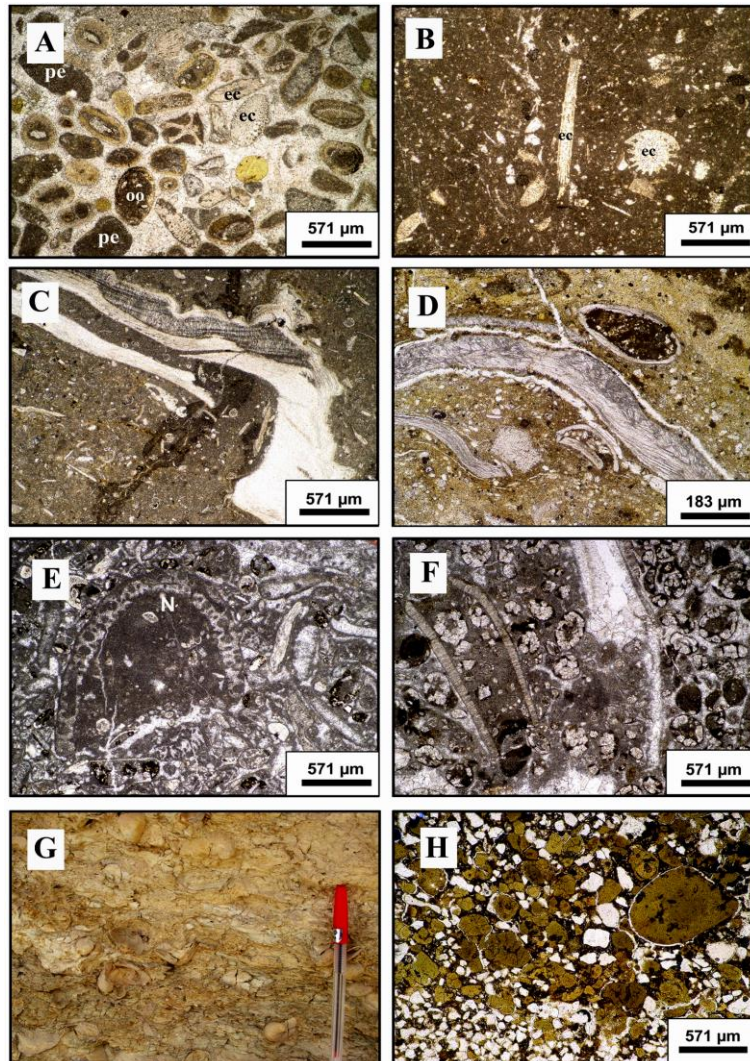


Fig. 10: **A.** Thin-section photomicrograph showing the oolitic peloidal grainstone that consists of echinodermal fragments (ec), oolites (oo) and peloids (pe). The cement between the allochems is sparry calcite crystals. Gebel Shabraweet. Ordinary light. **B.** Thin-section photomicrograph showing the molluscan-echinoidal wackestone. The rock consists of echinodermal particles (ec) and shell debris embedded in dark lime mud matrix. Gebel Shabraweet. Ordinary light. **C.** Thin-section photomicrograph showing the bioclastic foraminiferal wackestone that is composed of oyster fragments and planktonic forams scattered in a micritic matrix. The Northern Galala. Ordinary light. **D.** Thin-section photomicrograph showing the ostracoda molluscan packstone. The main allochems are the oysters, ostracods and planktonic forams. Notice: the clear calcite rims around the oyster particle. The Northern Galala. Ordinary light. **E.** Thin-section photomicrograph showing the dolomitic algal bioclastic packstone. It is built up of oyster, echinodermal and algal fragments. The algal particles may be *Neomeris* sp. (N). The Southern Galala. Ordinary light. **F.** Thin-section photomicrograph showing the dolomitic peloidal packstone. The allochems are represented by peloids, algal fragments, oysters and foraminiferal bioclasts scattered in a micritic matrix. Notice: the peloids are replaced selectively by dolomite rhombs from borders to centers. The Southern Galala. Ordinary light. **G.** Field photograph showing an oyster embankment in the limestone of the Galala Formation exposed at the Northern Galala. **H.** Thin-section photomicrograph the sandy dolomitic glauco-arenite that consists of well-rounded green glauconite pellets, quartz grains cemented together by ferroan dolomitic cement. The Southern Galala. Ordinary light.

These limestones are massive tightly-packed packstones enriched in oyster shell hash (Figs.10G). Other bioclasts are mainly the echinoderms and ostracods.

The co-existence of oysters and the foreigner planktonic foraminifera and ammonites in the oyster claystones of the Northern and Southern Galalas suggests deeper and high energetic conditions. Accordingly, oyster claystone embankment represents a skeletal biotope, developed by storm and waves in a deep shallow subtidal environment. The oyster limestone embankments represent biostormal banks since they have been formed by reworking processes under the effect of moderate to high energetic conditions and significant carbonate production in the shallow subtidal setting (Burchette and Wright 1992). The slightly restricted biota suggests that these banks represent shallow subtidal bioherms (Read 1980). The fragmentary nature of the oyster shells suggests turbulence during deposition (Harris et al. 1997). Aigner (1982) revealed that the large fossil lags embedded within mud matrix are a consequence of episodic storm induced erosion and re-deposition. Such facies is analogous to SMF-12 of Wilson (1975).

3- Deep subtidal facies:

The deep subtidal facies is typified by the glauco-arenite. This lithofacies is recorded only from one bed (1 m) at the lower part of the Southern Galala. Rock belonging to this lithofacies is reddish green, sandy, dolomitic and ferruginated. They consist of green glauconite, quartz grains and phosphatic fragments cemented by ferroan dolomite cement (Figs.10H). The glauconites are probably produced as a result of alteration of different minerals (clay minerals, mica and feldspars) that provide K and Fe in a local reducing environment (Genedi 1998). The presence of glauco-arenite suggests that a deep subtidal condensed facies was formed under the effect of both the subsidence and the low sedimentation rates (Buchbinder et al. 2000). They were accumulated in an open marine deep shelf areas characterized by slow rate of deposition with anoxic conditions and upwelling currents (Harris et al. 1997 and El-Azabi et al. 1998). The authigenic glauconite is interpreted to be deposited in deep subtidal environments (Marquis and Laury 1989 and Mesaed 1999). Similar glauconitic arenite was recognized from the Cenomanian Galala Formation of the Southern Galala by Mansour et al. (2001).

DEPOSITIONAL HISTORY

The deposition of the Cenomanian rocks (Galala Formation) represents the first Late Cretaceous transgression in the north Eastern Desert (Mansour et al. 2001). Issawi and Osman (2000) reported that the Cenomanian transgression becomes shallower as going southward in the Egyptian territories. Ahmed (2004) stated that during the Late Cenomanian times, a marine transgression took place over a widespread shelf areas resulted in deposition of the Galala Formation in the north Eastern Desert in form of shallowing-upward cycles. The numerous oyster-bearing strata within the studied sequence of the Galala Formation reflect the evolving sea-level rise of the Cenomanian Sea which corresponds to the Tethyan-highstand. The Galala Formation was deposited during a long-term transgressive phase of the shallow Cenomanian Sea that is intermittent with short-term regressive periods. The Cenomanian transgression advanced gradually from the north to the south throughout the study area. The transgression of the Cenomanian Sea over the study area corresponds to the global sea-level rise of Flexer et al. (1986) except for the local tectonic periods. Kora et al. (2001a) revealed that the transgression of the Cenomanian Sea over the north Eastern Desert of Egypt is consistent with the global sea-level highstand of Haq et al. (1987) that have started from about 95.5 M.Y ago.

The litho-, bio- and microfacies associations of the Galala Formation and their lateral facies change indicate that the sedimentary environment of the Galala Formation was that of a clastic-carbonate homoclinal shallow ramp setting as indicated by: 1) Lack of a detectable shelf break or slope facies. 2) Lack of a reefal margin. 3) The prevalence of the peritidal to open marine shallow subtidal facies. 4) A biological association dominated by bivalves, echinoderms, gastropods and ostracods. 5) The growth of discrete oyster embankments, which are flourished under the effect of the increasing in the rate of sea-level rise. 6) The currency of the transgressive and highstand deposits.

The vertical and lateral facies variation of the Galala Formation monitors the gradual transition from the proximal inner to distal mid ramp settings (Fig.11). This ramp facies is divided herein into the following environments: 1) Inner and/or proximal ramp at Gebel El-Zeit. 2) Mid ramp at the Southern and Northern Galalas, Gebel Ataqa and Gebel Shabraweet. It exhibits an intra-ramp basin at the Southern Galala and a carbonate buildup at Gebel Ataqa. The Southern and Northern Galalas, Gebel Ataqa and Gebel Shabraweet were separated by the east-west faults. The east-west oriented faults were initially formed during the Late Triassic/Jurassic extension related to the drifting of the African/Arabian Plates away from the Eurasian Plate as a result of opening of the Neotethyan Sea (Hussein and Abd Allah 2001). The outer ramp to basin settings is not detected within the study area. They seem to have been encountered in the Cenomanian of northern Sinai, where they are represented by the subsurface, hemipelagic chalky facies (Ayyad and Darwish 1996).

The facies changes and the variation of thickness of the shallow ramp deposits of the Galala Formation are depending mainly upon the sea-level changes and the synsedimentary local tectonic uplift and subsidence. In general, the sea-level rise is responsible for deposition of the subtidal facies. With lowering of the sea-level, the peritidal facies was deposited. The extreme sea-level drop leads to the development of the coastal plain shoreface clastics and subaerial facies. The sea-level rise of the Cenomanian Sea is also implied by the presence of oyster-bearing strata overlying the fluvial-fluviomarine clastic facies of the Early Cretaceous Malha Formation. A marked regression was recognized at the topmost part of the Galala Formation as evidenced by the presence of subaerial facies (i.e. caliche) at the topmost part of

Gebel El-Zeit, the Northern Galala and Gebel Ataqa and by the siliceous ferruginated dolomicrite lithofacies at the topmost part of Gebel Shabraweet (Figs.2 & 5-8)

During the lowstand periods of sea level, the ramp (Gebel El-Zeit) was exposed, hence the continental run-off by local rivers transported the siliciclastic sediments towards the lowstand shorelines. This decreases the carbonate production on the proximal part of the ramp. During the transgressive and highstand periods of the sea, the ramp passes through two stages; the evolution of siliciclastic-carbonate ramp facies at the Southern and Northern Galalas and the establishment of a dominated carbonate ramp facies at Gebel Ataqa and Gebel Shabraweet. Both stages represent a mid ramp setting.

The proximal inner ramp clastic-dominated facies corresponds to a tectonic stable period during which sedimentation rate kept pace with subsidence. The source of these clastics is positioned southward. The presence of plant remains within the succession of the Galala Formation at Gebel El-Zeit characterizes the coastal marine proximal ramp environment of warm and humid climate.

The drowning of the ramp in the central part of the study area is resulted from a local tectonic subsidence that leads to form an "intra-ramp basin" at the Southern Galala. This contributes to an increase in water depth and then a flooding is happened as the rate of sea-level rise is greater than the rate of carbonate sedimentation and this result in an open marine clastic-carbonate, shallow subtidal facies inter-fingering with deeper facies as indicated by the highly-diverse faunal content and the presence of ammonites and planktonic foraminifera-bearing strata. The change from the clastic-dominated facies of Gebel El-Zeit to the mixed clastic-carbonate facies of the Southern and Northern Galalas reflects a regional rise in sea level, whereas the rise of sea level diminishes the clastic area and led to flooding of coastal areas by carbonate facies.

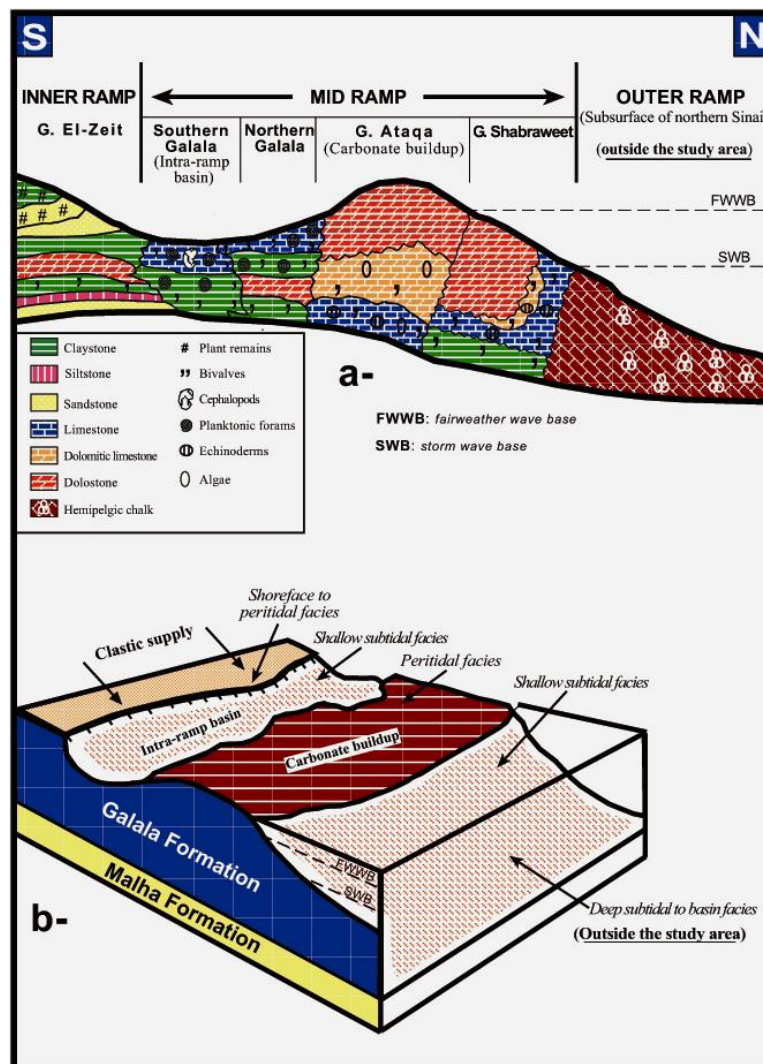


Fig.11: Schematic diagram shows: a. Depositional model of the siliciclastic-carbonate ramp of the Galala Formation. b. General depositional facies of the Galala Formation.

The Northern part of the study area was uplifted with a remarkable sea-level drop and hence the peritidal facies dominates near the mean sea level. This tectonic uplifting is synchronous with the low-lying area on which the intra-ramp basin facies was deposited. The lack of siliciclastics within the succession of Gebel Ataqa reflects the increase of the

carbonate sedimentation at the expense of the claystones under the effect of uplifting. This uplifting leads to forming of isolated carbonate buildup at Gebel Ataqa, where the succession is composed mainly of shallowing-upward, pure carbonate, shallow subtidal and peritidal cycles developed on the mid ramp. This isolated buildup is developed when the rate of the sediment production of the buildup exceeds the rate of sea-level rise (Burchette and Wright 1992).

The gradual transition from the intra-ramp basin at the Southern Galala passing through the transitional facies at the Northern Galala to the carbonate buildup at Gebel Ataqa represents a shift from the fine siliciclastic dominant and mixed siliciclastic-carbonate facies to carbonate dominant sedimentation. This transition reflects the shallowing and infilling of the intra-ramp basin and the progradation of the carbonate buildup at Gebel Ataqa. Carbonate buildup facies of Gebel Ataqa is closely similar to that found on the ramp by Markello and Read (1981). The dominance of carbonates (82%) over the claystones (18%) in the lithofacies of Gebel Shabraweet reflects a period of elevation but with deeper conditions than Gebel Ataqa.

REFERENCES

- Abdel Gawad GI, El-Qot GM and Mekawy, MS, 2007, Macrobiostratigraphy of the Upper Cretaceous succession from Southern Galala, Eastern Desert, Egypt. 2nd Inter Conf Geo Tethys Cairo Univ 2: 329-449.
- Abdel Shafy E, Ibrahim N, Ied, IM, 2002, Micro bio- and chronostratigraphy of the Upper Cretaceous rocks in the north-central part of the Gulf of Suez area, Egypt. *Egy J Geol* 46/2: 535-558.
- Ahmed HA, 2004, Stratigraphy and sedimentology of the Upper Cretaceous/Lower Tertiary successions in the Southern Galala Plateau, Eastern Desert, Egypt. Ph D Thesis Al-Azhar Univ: 300 p.
- Ahr WM, 1973, The carbonate ramp-an alternative to the shelf model. *Trans Gulf Coast Assoc Geol Soc* 23: 221-225.
- Aigner T, 1982, Event stratification in nummulites accumulations and in shell beds from the Eocene of Egypt. In: Einsele G & Seilacher A (Eds.): *Cyclic and event stratification* Springer Verlag Berlin: 248-262.
- Al-Aasm IS & Packard JJ, 2000, Stabilization of early-formed dolomite: a tale of divergence from two Mississippian dolomites. *Sed Geol* 131: 97-108.
- Al-Ahwani MM, 1982, Geological and sedimentological studies on Gebel Shabraweet area, Suez Canal district, Egypt. *Ann Geo Surv Egypt* XII: 305-381.
- Aurell M, 1991, Identification of systems tracts in low-angle carbonate ramps: examples from the Upper Jurassic of Iberian Chain (Spain). *Sed Geol* 73: 101-115.
- Awad GH, Abdallah AM, 1966, Upper Cretaceous in Southern Galala, Eastern Desert with emphasis on neighbouring areas. *J Geol UAR* 10 (2): 125-144.
- Ayyad MH, Darwish M, 1996, Syrian Arc Structures: a unifying model of inverted basins and hydrocarbon occurrences in north Egypt. In: *Proceed 14th Conf EGPC Pet Expl Prod Cairo*: 40-59.
- Bádenas B, Aurell M, 2001, Proximal-distal facies relationships and sedimentary processes in a storm dominated carbonate ramp (Kimmeridgian, northwest of the Iberian Ranges, Spain). *Sed Geol* 139: 319-340.
- Barthel KM, Herrmann-Degen W, 1981, Late Cretaceous and Early Tertiary stratigraphy in the Great Sand Sea and its SE margins (Farafra and Dakhla Oases), SW Desert, Egypt. – *Mitt Bayer Staatssl Paläont Hist Geol* 21: 141-182.
- Bauer J, Kuss J, Steuber T, 2002, Platform environments, microfacies and system tracts of the Upper Cenomanian-Lower Santonian of Sinai, Egypt. *Facies* 47: 1-26.
- Blatt H, 1982, *Sedimentary petrology*. W.H. Freeman San Francisco California: 564 p.
- Bosworth W, Guiraud R, Kessler LG, 1999, Late Cretaceous (ca. 84 Ma) compressive deformation of the stable platform of northeast Africa (Egypt): far-field stress effect of the "Santonian Event" and origin of the Syrian Arc deformation belt. *Geology* 27: 633-636.
- Braithwaite CJR, Talbot MR, 1972, Crustacean burrows in the Seychelles, Indian Ocean. *Paleogeog Paleoclim Paleoeoc* 11: 265-285.
- Buchbinder B, Benjamini C, Lispon-Benitah S, 2000, Sequence development of the Late Cenomanian-Turonian carbonate ramps, platforms and basins in Israel. *Cret Res* 21: 813-843.
- Burchette TP, Wright VP, 1992, Carbonate ramp depositional systems. *Sed Geol* 79: 3-57.
- Bauer J, Kuss J, Steuber T, 2003, Sequence architecture and carbonate platform configuration (Late Cenomanian-Santonian), Sinai, Egypt. *Sedimentology* 50: 387-414.
- Bauer J, Marzouk AM, Steuber T, Kuss J, 2001, Lithostratigraphy and biostratigraphy of the Cenomanian-Santonian strata of Sinai, Egypt. *Cret Res* 22: 497-526.
- Camion GF, 1991, Sedimentologic and paleotectonic evolution of carbonate platforms on a segmented continental margin: example of the African Tethyan margin during and early Senonian times. *Paleogeog Paleoclim Paleoeoc* 87: 29-52.
- Dickson JAD, 1966, Carbonate identification and genesis as revealed by staining. *J Sed Pet* 36: 491-505.
- El-Akkad S, Aballah, AM, 1971, Contribution to geology of Gebel Ataqa. *Ann Geol Surv Egypt* 1: 21-42.
- El-Araby A, 2002, Depositional sequences in shallow carbonate-dominated sedimentary systems- An example from the Cenomanian Halal Formation, Gabal Halal, North Sinai, Egypt. 6th Inter Conf Geol Arab World Cairo Univ: 655-676.
- El-Ayaat A, Khalifa, MA, 2010, Lithostratigraphy, facies analysis, paleoenvironments and cyclicity of the upper Cretaceous (Cenomanian-Santonian) mixed carbonate-siliciclastic sequence in north Eastern Desert, Egypt. 5th Inter Conf Geol Tethys Realm South Valley Univ: 421-444

- El-Azabi MH, Al-Maleh AK, Yzbek, MK, 1998, Facies characteristics and depositional environments of Maastrichtian-Paleocene succession in Jabal El-Bardeh and Jabal Anter, Kasr Al Heir-Turfa area, Southern Palmyridian region, Syria. *MERC Ain Shams Univ Earth Sci Ser* 12: 1-20.
- El-Hawat AS, 1997, Sedimentary basins of Egypt. An overview of dynamic stratigraphy In: African basins (Ed. R. C. Selley) *Sedimentary basins of the world* 3: 39-85. Elsevier, Amsterdam.
- Elrick M, 1995, Cyclostratigraphy of Middle Devonian carbonates of the Eastern Great Basin. *J Sed Res* B65 (1): 61-79.
- Elrick M, Read JF, 1991, Cyclic ramp-to-basin carbonate deposits, Lower Mississippian, Wyoming and Montana: A combined field and computer modeling study. *J Sed Pet* 61 (7): 1194-1224.
- Enos P, 1983, Shelf, in: Scholle PA, Bebout DG and Moore C, eds. carbonate depositional environments. *Amer Assoc Pet Geol Mem* 33: 267-296.
- Evans K, Rowell AJ, Rees MN, 1995, Sea-level changes and stratigraphy of the Nelson limestone (Middle Cambrian). Neptune range, Antarctica. *J Sed Res* B65 (1): 32-43.
- Flexer A, Rosenfeld A, Lispon-Benitah S, Honigstein A, 1986, Relative sea level changes during the Cretaceous in Israel. *Amer Assoc Pet Geol Bull* 70 (11): 1685-1699.
- Flügel E, 1982, *Microfacies analysis of limestones*. Springer-Verlag Berlin-Heidelberg-New York, 633 p.
- Gawthorpe RL, 1986, Sedimentation during carbonate ramp-to-slope evolution in a tectonically active area: Bowland Basin (Dinantian), northern England. *Sedimentology* 33: 185-206.
- Genedi A, 1998, Comparative study of facies and mineral composition of the Cenomanian sediments in northeast and southwest Sinai, Egypt. *Egy J Geol* 42/2: 575-596.
- Ghorab, MA, 1961, Abnormal stratigraphic features in Ras Gharib Oil Field, Egypt. *3rd Arab Pet Cong Alexandria Egypt* 10 p.
- Grosheny D, Malartre F, 2002, Reconstruction of outer shelf paleoenvironments in the Turonian-Coniacian of southeast France (micropaleontology-sedimentology): local and global controlling factors. *Marine Micropaleontology* 47: 117-141.
- Guiraud R, Bosworth W, 1997, Senonian basin inversion and rejuvenation of rifting in Africa and Arabia: synthesis and implication to plate-scale tectonics. *Tectonophysics* 282: 39-82.
- Guiraud R, Issawi B, Bosworth W, 2001, Phanerozoic history of Egypt and surrounding areas. In: PA Ziegler, W Cavazza, AHF Robertson & S Crasquin-Soleau (eds). *Peri-Tethys Mem* 6: Peri-Tethyan Rift/Wrench basins and passive margins. *Mem Mus Nat Hist Nature* 186: 469-509.
- Haq BU, Hardenbol J, Vail PR, 1987, Chronology of fluctuating sea levels since the Triassic. *Science* 235:1156-1167.
- Harris MK, Thayer PA, Amidon, MB, 1997, Sedimentology and depositional environments of Middle Eocene terrigenous-carbonate strata southwestern Atlantic Coastal Plain, U.S.A. *Sed Geol* 108: 141-161.
- Hofmann A, Dirks HGM, Jelsma HA, 2004, Shallowing-upward carbonate cycles in the Belingure Belt, Zimbabwe: A record of Archean sea-level oscillations. *J Sed Res* 74 (1): 64-81.
- Hussein M, Abd Allah AMA, 2001, Tectonic evolution of the northeastern part of the African continental margin, Egypt. *J Afr Earth Sci* 33 (1): 49-68.
- Ismail AA, Akarish AIM, 2000, Stratigraphy and facies analysis of some Cenomanian-Turonian exposures in the North Eastern Desert, Egypt. *Egy J Geol* 44 (2): 277-294.
- Issawi B, Osman R, 2000, Upper Cretaceous-Lower Tertiary platform-ramp environments in northern Egypt. *5th Conf Geol Arab World (GAW5) Cairo Univ*: 1289-1308.
- Keller M, 1997, Evolution and sequence stratigraphy of Early Devonian carbonate ramp, Cantabrian Mountains, Northern Spain. *J Sed Res* 67 (4): 638-652.
- Khalifa MA, Abu El-Ghar MS, Helal SA, Hussein AW, 2004, Depositional history of the Lower Eocene drowned carbonate platform (Drunka Formation), west of Assiut-Minia stretch, Western Desert, Egypt. *7th Inter Conf Geol Arab World (GAW.7) Cairo Univ*: 233-254.
- Khalifa MA, El-Ayyat AM, 2007, Facies and sequence stratigraphy of the Cenomanian Galala Formation at Gebel Zeit area, Gulf of Suez, Egypt. *Assiut Univ J Geol* 36 (1): 1-49.
- Khalifa MA, Kandil AA, 2004, Contribution to the lithostratigraphy and depositional history of the Upper Cretaceous rock units, Northern Galala, Eastern Desert, Egypt. *Ann Geol Surv Egypt XXVII*: 213-235.
- Kora M, Khalil H, Sobhy M, 2001a, Cenomanian-Turonian macrofauna from the Gulf of Suez region: Biostratigraphy and Paleobiogeography. *Egy J Geol* 45/1: 441-462.
- Kora M., Khalil H, Sobhy M, 2001b, Stratigraphy and microfacies of some Cenomanian-Turonian succession in the Gulf of Suez region, Egypt. *Egy J Geol* 45/1: 413-439.
- Kuss J, 1992, Facies and stratigraphy of Cretaceous limestones from Northeast Egypt, Sinai and Southern Jordan. *1st Conf Geol Arab World (GAW1) Cairo Univ* 283-301.
- Kuss J, Malchus N, 1989, Facies and composite biostratigraphy of Late Cretaceous strata from Northeast Egypt. In: WIEDMANN, J (Eds.) *Cretaceous of the Western Tethys Proc 3rd Inter Cretaceous Symp Tubigen 1987*: 879-910. E. Schweizerbart'sche Verlagsbuch-handlung Stuttgart.
- Lakew T, 1990, Microfacies and cyclic sedimentation of the Upper Triassic Cakcare di zu (Southern Alps). *Facies* 22: 187-232.

- Lonnee J, Al-Aasm IS, 2000, Dolomitization and fluid evolution in the Middle Devonian Sulphur Point Formation, Rainbow South Field, Alberta: Petrographic and geochemical evidence. *Bull Can Pet Geol* 48 (3): 262-283.
- Lüning S, Kuss J, Bachmann M, Marzouk, AM, Morsi, AM, 1998a, Sedimentary response to basin inversion: Mid-Cretaceous-Early Tertiary Pre-to syndeformational deposition at the Areif El Naqa anticline (Sinai, Egypt). *Facies* 38: 103-136.
- Lüning S, Marzouk AM, Morsi AM, Kuss J, 1998b, Sequence stratigraphy of the Upper Cretaceous of Central east Sinai, Egypt. *Cret Res* 19: 153-196.
- Mansour HH, El-Younsy ARM, Ahmed EA, Tobschall HJ, Shaheen MAM, 2001, Facies and sedimentological evolution of the pre-rift cretaceous-Lower Tertiary sequence southeast Southern Galala, Gulf of Suez, Egypt. 2nd Inter Conf Geol Africa I: 421-447.
- Markello JR, Read JF, 1981, Carbonate ramp-to-deeper shale shelf transitions of an Upper Cambrian intrashelf basin, Nolichucky Formation, southwest Virginia, Appalachians. *Sedimentology* 28: 573-597.
- Marquis SAJR, Laury RL, 1989, Glacio-eustasy, depositional environments, diagenesis and reservoir characters of Goen limestone cyclothem (Desmoinesian), Concho platform, Central Texas. *Amer Assoc Pet Geol Bull* 73 (2): 166-181.
- Mesaed AA, 1999, Origin and fabric evolution of the Eocene glaucony of the northern part of the Western Desert, Egypt. *Egy J Geol* 43/2: 29-54.
- Metwally MHM, Abd El-Azeam S, Shahat W, 1995, Microfacies and environmental development of the Upper Cretaceous formations, Southern Galala, Gulf of Suez, Egypt. *Bull Fac Sci Zagazig Univ* 17 (2): 11-39.
- Nishikawa T, Ito M, 2000, Late Pleistocene barrier-island development reconstructed from genetic classification and timing of erosional surfaces, Paleo-Tokyo Bay, Japan. *Sed Geol* 137: 25-42.
- Norton P, 1967, Rock stratigraphic nomenclature of the Western Desert. Unpubl Rep Pan American Oil Co UAR Cairo Egypt
- Olsen TR, Mellere D, Olsen T, 1999, Facies architecture and geometry of landward-stepping shoreface tongues: the Upper Cretaceous Cliff House Sandstone (Mancos Canyon, south-west Colorado). *Sedimentology* 46: 603-625.
- Pomar L, 2001, Types of carbonate platforms: a genetic approach. *Basin Res* 13: 313-334.
- Puga-Bernabéu Á, Braga JC, Martín JM (2007) High-frequency cycles in Upper-Miocene ramp-temperate carbonates (Sorbas Basin, SE Spain). *Facies* 53: 329-345.
- Read JF, 1980, Carbonate ramp to basin transitions and foreland basin evolution, Middle Ordovician, Virginia Appalachians. *Amer Assoc Pet Geol Bull* 64: 1575-1612.
- Read JF, 1985, Carbonate platform facies models. *Amer Assoc Pet Geol Bull* 66: 860-878.
- Reading HG, 1996, Sedimentary environments: processes, facies and stratigraphy. Blackwell Sci. Ltd (3rd edition). Chapter 9: 325-394.
- Said R, 1962, The geology of Egypt. Elsevier Publ Amsterdam, London, New York: 377 p.
- Said R, 1971, Explanatory notes to accompany the geological map of Egypt. *Geol Surv Egypt* 56, 123 p, Cairo.
- Sanders D, Höfling R, 2000, Carbonate deposition in mixed siliciclastic-carbonate environments on top of an organic wedge (Late Cretaceous, Northern Calcareous Alps, Austria). *Sed Geol* 137: 127-146.
- Schulze F, Kuss J, Marzouk A, 2005, Platform configuration, microfacies and cyclicities of the Upper Albian to Turonian of west central Jordan. *Facies* 50: 505-527.
- Shinn EA, 1983, Tidal flat environment. In: Scholle, PA, Bebout, DG, Moore, CH (Eds.), Carbonate depositional environments, 33, *Amer Assoc Pet Geol Mem*: 173-210.
- Tucker ME, Wright VP, 1990, Carbonate sedimentology. Blackwell Sci Publ Oxford London 482 p.
- Tucker ME, Calvet F, Hunt D, 1993, Sequence stratigraphy of carbonate ramps: system tracts, models and application to the Muschelkalk carbonate platforms of Eastern Spain. *Spec Publ Inst Assoc Sediment* 18: 397-415.
- Wanas HA, 2008, Cenomanian rocks in the Sinai Peninsula, Northeast Egypt: Facies analysis and sequence stratigraphy. *J Afr Earth Sci* 52: 125-138.
- Warren JK, 2000, Dolomite: occurrence, evolution and economically important associations. *Earth Sci Rev* 52: 1-81.
- Wilkinson BH, Drunnon CN, Rothman ED, Diedrich NW, 1997, Stratal order in peritidal carbonate sequences. *J Sed Res* 67 (6): 1068-1082.
- Wilson JL, 1975, Carbonate facies in geologic history. Springer-Verlag, Berlin, Heidelberg, New York, 471 p.
- Wray JL, 1977, Calcareous algae. Elsevier Scientific Publishing Co., Amsterdam, Oxford, New York, 185 p.
- Wright VP, 1986, Facies sequences on a carbonate ramp: the Carboniferous limestone of South Wales. *Sedimentology* 33: 221-241.
- Youssef EAA, Khalifa MA, Abdel Fattah MA, Refaat AA, 2002, Sequence stratigraphy of the Late Paleocene-Early Eocene carbonate ramp: Southern Galala Plateau, Eastern Desert, Egypt. 6th Inter Conf Geol Arab World (GAW.6), Cairo Univ: 521-534.